transporter. Perhaps these pathways are used when bacteria are exposed to the complex molecular content of intracellular organelles of host cells or potentially nutrient-rich biofilms. *Legionella* is reportedly auxotrophic for several amino acids, so it was surprising to find potential genes for their synthetic pathways: cysteine from pyruvate or serine, methionine from cysteine, and both phenylalanine and tyrosine from phosphoenolpyruvate. Even if some of these genes are not expressed under laboratory growth conditions, their presence presumably relates to the organism's ability to persist in diverse environments.

In addition to previously recognized virulence factors (table S5), we identified new candidates (table S6), including homologs of genes encoding virulence functions in other bacteria. Moreover, ~145 apparent secreted or membrane proteases and other hydrolases, some of which may function as virulence factors, exist in *L. pneumophila*. Among fully sequenced organisms, this is exceeded only by the predatory *Bdellovibrio* (*22*). *L. pneumophila* has been proposed to utilize bacterial-induced apoptotic (early) and/or necrotic pore-forming (late) events to exit infected hosts (*23*); its putative hydrolases may be involved in these processes.

The genome sequence of *L. pneumophila* offers the opportunity to explain its broad host range and extraordinary ability to resist eradication in water supplies. Having lists of genes unique to *Legionella* or shared with unrelated bacteria with similar life-styles, it should now be possible to determine experimentally which of them distinguish *Legionella* species displaying different host preferences or pathogenicity.

References and Notes

1. D. W. Fraser *et al.*, *J. Med.* **297**, 1189 (1977).
2. B. S. Fields, R. F. Benson, R. E. Besser, *Clin. Microbiol. Rev.* **15**, 506 (2002).
3. D. S. Zamboni, S. McGrath, M. Rabinovitch, C. R. Roy, *Mol. Microbiol.* **49**, 965 (2003).
4. T. Zusman, G. Yerushalmi, G. Segal, *Infect. Immun.* **71**, 3714 (2003).
5. H. Nagai, J. C. Kagan, X. Zhu, R. A. Kahn, C. R. Roy, *Science* **295**, 679 (2002).
6. Z.-Q. Luo, R. R. Isberg, *Proc. Natl. Acad. Sci. U.S.A.* **101**, 841 (2004).
7. J. Chen *et al.*, *Science* **303**, 1358 (2004).
8. H. Nagai, C. R. Roy, *Cell. Microbiol.* **5**, 373 (2003).
9. Supporting materials are available on *Science* Online.
10. Additional details are at http://legionella.cu-genome.org/annotation/annotation.html.
11. K. Suwwan de Felipe, S. Pampou, S. Kalachikov, H. A. Shuman, unpublished data.
12. G. Segal, M. Purcell, H. A. Shuman, *Proc. Natl. Acad. Sci. U.S.A.* **95**, 1669 (1998).
13. J. P. Vogel, H. L. Andrews, S. K. Wong, R. R. Isberg, *Science* **279**, 873 (1998).
14. G. Segal, J. J. Russo, H. A. Shuman, *Mol. Microbiol.* **34**, 799 (1999).
15. A. K. Brassinga *et al.*, *J. Bacteriol.* **185**, 4630 (2003).
16. S. Sturgill-Koszycki, M. S. Swanson, *J. Exp. Med.* **192**, 1261 (2000).
17. S. L. Cirillo, J. Lum, J. D. Cirillo, *Microbiology* **146**, 1345 (2000).
18. R. Seshadri *et al.*, *Proc. Natl. Acad. Sci. U.S.A.* **100**, 5455 (2003).
19. G. Fernandez-Leborans, Y. Olalla Herrero, *Ecotoxicol. Environ. Saf.* **47**, 266 (2000).
20. D. De Biase, A. Tramonti, F. Bossa, P. Visca, *Mol. Microbiol.* **32**, 1198 (1999).
21. J. R. George, L. Pine, M. W. Reeves, W. Knox Harrell, *J. Clin. Microbiol.* **11**, 286 (1980).
22. S. Rendulic *et al.*, *Science* **303**, 689 (2004).
23. L. Y. Gao, Y. Abu Kwaik, *Environ. Microbiol.* **2**, 79 (2000).

24. We thank M. Horwitz (UCLA School of Medicine, Los Angeles, CA) for supplying the Philadelphia 1 bacterial stock used in this study. We are especially grateful to I. S. Edelman for his constant encouragement during the course of this project. Large-scale analyses were aided by the availability of software and hardware from the Bioinformatics Core Facility sponsored by the AMDeC Foundation, Inc. This work was supported by NIH grants U01 1 AI 4437 (J.J.R.) and AI 23549 (H.A.S.), a Packard Fellowship for Science and Engineering (J.J.), and funds generously provided by the Columbia Genome Center. S.M.G. is supported by a grant from the Pasteur Foundation of New York.

Supporting Online Material

www.sciencemag.org/cgi/content/full/305/5692/1966/DC1
Materials and Methods
SOM Text
Tables S1 to S6
Figs. S1 to S6

30 April 2004; accepted 9 August 2004

Nitric Oxide Represses the *Arabidopsis* Floral Transition

Yikun He,[1,2]* Ru-Hang Tang,[1]* Yi Hao,[1]* Robert D. Stevens,[3] Charles W. Cook,[1] Sun M. Ahn,[1] Liufang Jing,[1] Zhongguang Yang,[4] Longen Chen,[4] Fangqing Guo,[5] Fabio Fiorani,[1]† Robert B. Jackson,[1] Nigel M. Crawford,[5] Zhen-Ming Pei[1]‡

The correct timing of flowering is essential for plants to maximize reproductive success and is controlled by environmental and endogenous signals. We report that nitric oxide (NO) repressed the floral transition in *Arabidopsis thaliana*. Plants treated with NO, as well as a mutant overproducing NO (*nox1*), flowered late, whereas a mutant producing less NO (*nos1*) flowered early. NO suppressed *CONSTANS* and *GIGANTEA* gene expression and enhanced *FLOWERING LOCUS C* expression, which indicated that NO regulates the photoperiod and autonomous pathways. Because NO is induced by environmental stimuli and constitutively produced, it may integrate both external and internal cues into the floral decision.

The life of flowering plants is divided into two distinct phases, an initial vegetative phase during which meristems produce leaves and a subsequent reproductive phase during which meristems produce flowers. Genetic studies of the timing of flowering in *Arabidopsis* have revealed four major pathways (*1*). The photoperiod and vernalization pathways integrate external signals into the floral decision, whereas the autonomous and gibberellin (GA) pathways act independently of environmental cues (*2*).

NO plays a pivotal role in animals and has emerged as a key growth regulator in plants (*3*, *4*). NO promotes leaf expansion, inhibits maturation and senescence, stimulates light-dependent germination, and promotes deetiolation (*5*, *6*). Excess endogenous NO reduces growth and delays development in tobacco plants (*7*). NO production is induced by biotic and abiotic stimuli, such as drought, salt stress, and pathogen infection (*4*). In addition, substantial NO is emitted from plants into the atmosphere. Conversely, atmospheric NO, a major greenhouse pollutant produced by combustion of fossil fuels, can affect plants. Thus, NO has a central role in coordinating plant growth and development with environmental conditions. However, little is known about the molecular mechanisms underlying the function of NO in plants.

Treatment of *Arabidopsis* seedlings with an NO donor, sodium nitroprusside (SNP), enhanced vegetative growth and delayed flowering (Fig. 1). SNP increased shoot growth by ~65% at low concentrations (≤100 μM), although it inhibited growth at high concentrations (Fig. 1, A and B; fig S1A). The optimal SNP concentration for promoting shoot growth was ~100 μM. A similar promotive effect of

[1]Department of Biology, Duke University, Durham, NC 27708, USA. [2]Department of Biology, Capital Normal University, Beijing 100037, China. [3]Mass Spectrometry Laboratory, Duke University Medical Center, Research Triangle Park, NC 27709, USA. [4]Orthopaedic Research Laboratory, Duke University Medical Center, Durham, NC 27710, USA. [5]Division of Biological Sciences, University of California, San Diego, La Jolla, CA 92093, USA.

*These authors contributed equally to this work.
†Present address: Department of Plant Systems Biology, VIB-Ghent University, B-9052 Ghent, Belgium.
‡To whom correspondence should be addressed. E-mail: zpei@duke.edu

NO on chlorophyll content was also found (*8*). SNP delayed flowering in a dose-dependent manner, as measured by the increase in rosette leaf number and days to bolting—swift upward growth at the transition to flowering (Fig. 1, A, C, and D; fig. S1A). A standard indicator for flowering time is the number of leaves produced on the primary shoot before the first flower is initiated; plants that flower late form more leaves (*9*).

Exogenously applied NO may not replicate the function of endogenous NO and may have side effects in plants. Thus, analysis of genetic mutants with altered endogenous NO levels was conducted to determine the in vivo relevance of NO. An NO-hypersensitive screen for *NO overproducer* (*nox*) mutants in *Arabidopsis* was performed (*10*). NO inhibition of root growth was used as a phenotype for the initial screen (fig. S1B). Subsequently, NO production was measured with an NO-sensitive dye, 4,5-diaminofluorescein diacetate (*11*, *12*). Six *nox1* alleles were isolated (Fig. 2A; fig. S2) that contained high levels of NO in roots (*8*) and leaves (table S1) compared with wild type (WT) (Fig. 2B). The *nox1* mutant, which refers to *nox1-1* unless otherwise specified, showed the most root-growth hypersensitivity to SNP of all the mutants isolated. Mutants with altered NO biosynthesis or signaling have not yet been isolated via genetic screens, so *nox1* could provide a powerful tool for dissecting NO function. Despite recent identification of two types of NO synthase (NOS), pathogen-inducible iNOS and constitutive AtNOS, the sources of NO in plants remain to be fully elucidated (*4*, *11*, *12*).

NOX1 was identified as either very close or identical to *CUE1* by map-based cloning (fig. S3A). The morphological phenotype of *nox1* was almost identical to that described for *chlorophyll a/b binding protein* (*CAB*) *underexpressed 1* mutant (*cue1*), including small plant size and pale green leaves with a reticulate pattern (*13*). *CUE1* encodes a chloroplast phosphoenolpyruvate/phosphate translocator (*14*). Several lines of molecular genetic evidence demonstrated that *NOX1* is *CUE1* (fig. S3). The *cue1* mutants were hypersensitive to SNP and displayed an elevated

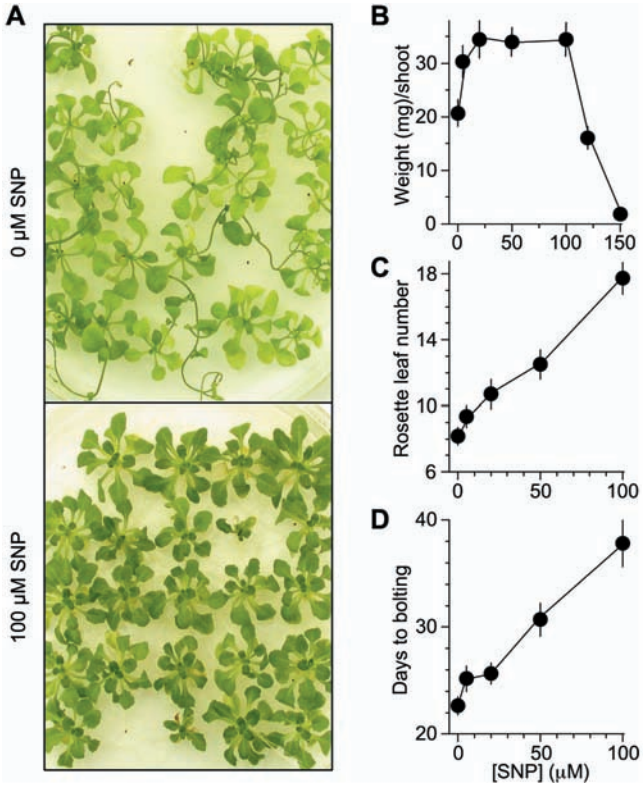

Fig. 1. Exogenous NO promotes vegetative growth but inhibits reproductive development. (**A**) The effects of an NO donor SNP on plant growth and development. *Arabidopsis* seedlings were grown in petri dishes containing SNP during long days (16-hour light/8-hour dark) for 5 weeks (*10*). (**B**) The effect of SNP concentration on shoot growth. (**C** and **D**) The effect of SNP on flowering times. Fresh weight per shoot (B), the rosette leaf number (C), and days to bolting (D) from experiments as in (A) and fig. S1A plotted as a function of the concentrations of SNP that were applied, respectively. Data from four separate experiments are presented (mean ± SD; n = 150 seedlings).

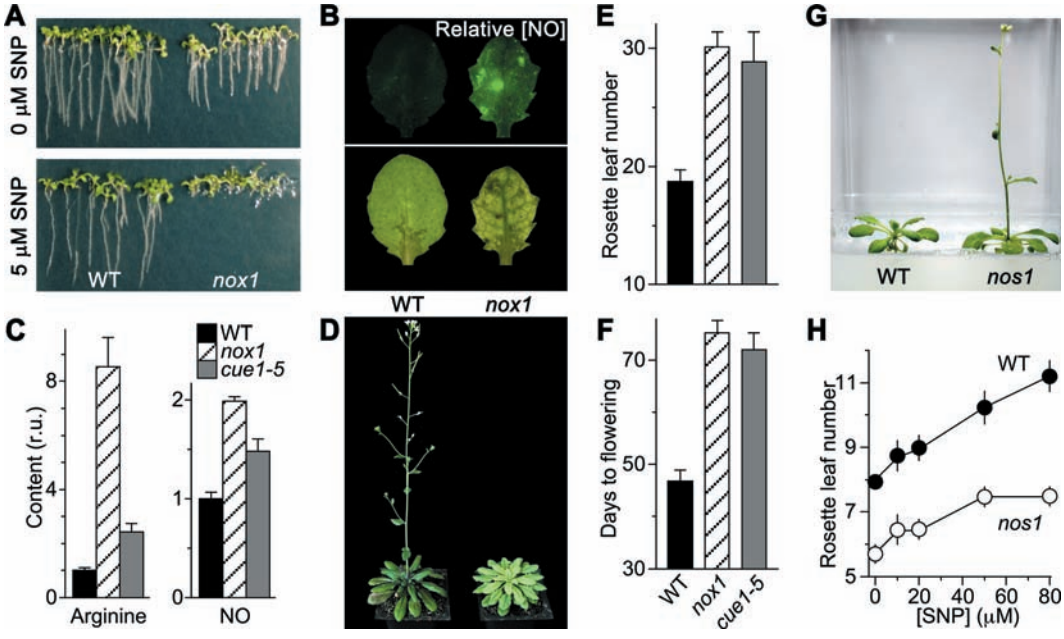

Fig. 2. Endogenous NO represses the floral transition. (**A**) The root growth phenotype in *nox1* mutant. (**B**) The endogenous NO levels in *nox1* and WT. Leaves were stained with DAF-2DA. Fluorescence was analyzed with excitation 490 nm and emission 515 nm (top) with the same exposure times (*10*). White-light images are shown at the bottom. (**C**) The levels of L-Arg and NO in WT, *nox1*, and *cue1-5*. Plants grown under 12-hour light/12-hour dark cycles were harvested 6 hours after dawn (*10*). The absolute levels of L-Arg and NO were 51.8 and 0.45 nmol per gram of fresh rosette leaves in WT, respectively. Values are normalized to those of WT. Each data point represents nine independent measurements (r.u., relative unit). (**D**) The *nox1* mutant flowers late. WT and *nox1* were grown in soil under 12-hour light/12-hour dark cycles and were photographed after 60 days of growth. (**E** and **F**) Flowering times of *nox1* and *cue1-5* mutants. The rosette leaf number (E) and days to flowering (F) from experiments as in (D) were scored (mean ± SD; $n \geq 25$ plants). (**G**) The *NO synthase 1* (*nos1*) mutant that produces fewer NO flowers early under long days. (**H**) The *nos1* mutant flowers earlier than WT under SNP treatments. Experiments similar to that in (G) were analyzed (mean ± SD; n = 20 to 30 plants).

level of endogenous NO. The *cue1* could not complement *nox1* phenotypes. In all six *nox1* alleles, the *CUE1* gene was deleted. Because NO is synthesized from the conversion of L-arginine (L-Arg) to L-citrulline (L-Cit) by NOS (*3*), free L-Arg and L-Cit are several-fold higher in *cue1* mutants than in WT plants (*14*), and *nox1* overproduces NO, we reasoned that disruption of the *CUE1* gene would increase the endogenous L-Arg concentration and thus would promote its conversion to NO. *nox1* and the *cue1-5* mutant harboring a single amino acid mutation (*14*) indeed exhibited larger amounts of L-Arg, L-Cit, and NO than WT (Fig. 2C; fig. S4), indicating that NOS-based NO production occurs in *Arabidopsis*.

Soil-grown *nox1* and *cue1* mutants showed a late-flowering phenotype (Fig. 2, D to F; table S1). This phenotype is not photoperiod-dependent, as *nox1* flowered late under all photoperiods. However, the phenotypic severity was influenced by photoperiods, with 18%, 61%, and 17% increases in the rosette leaf number seen under the light/dark (hours) cycles of 16/8, 12/12, and 8/16, respectively (table S1). This observation is consistent with the light-dependent phenotypes seen in *cue1* mutants (*13*).

In addition, we determined whether down-regulation of endogenous NO promotes the floral transition. The mutant *Atnos1* (*nos1*) that contains a reduced amount of NO (*11*) flowered earlier than WT (Fig. 2G), but still displayed sensitivity to SNP (Fig. 2H). The NO content of *nos1* plants was about 18% that of WT (*8*). The positive correlation between endogenous NO and the number of leaves produced indicates that NO may have a specific role in controlling the floral transition.

To test which components in the floral pathways are affected by NO, we analyzed expression of the floral meristem identity gene *LEAFY* (*LFY*). *LFY* is an important determinant in flower initiation, and its expression increases gradually before flowering commences (*15*). SNP suppressed *LFY* expression in a dose-dependent manner (Fig. 3, A and C). *LFY* expression was low in *nox1*, but was high in *nos1* plants compared with WT (Fig. 3, B and C). The negative correlation between *LFY* expression and endogenous NO suggests that NO repression of the floral transition is mediated, at least in part, by LFY.

Genetic epistasis studies have placed the genes that regulate the floral transition into four major pathways in *Arabidopsis*, all of which converge on the target *LFY* (*2*). The *nox1* mutants flowered late and showed a dwarf phenotype, resembling those of GA-deficient mutants (*16*). GA promoted flowering in *nox1* and WT plants but could not reverse the *nox1* dwarf phenotype (*8*), which suggests that NO may function in parallel with GA. Because *nox1* and mutants of the autonomous pathway flower late on both long and short days (*1*), we reasoned that *nox1* might affect this pathway. The vernalization and autonomous pathways converge on a floral repressor, *FLOWERING LOCUS C* (*FLC*), and late-flowering mutants of the autonomous pathway always have elevated *FLC* expression (*17*). Treatment with low concentrations (≤50 μM) of SNP decreased *FLC* expression, whereas high concentrations (>50 μM) increased *FLC* expression (Fig. 3, D and F). *FLC* expression was high in *nox1* and slightly reduced in *nos1* compared with WT (Fig. 3, E and F). The late-flowering phenotype observed in WT plants treated with high doses of SNP or in *nox1* may result from up-regulation of *FLC* expression. However, the late-flowering phenotype in plants treated with low doses of SNP may be caused by components independent of *FLC*. Nonetheless, the flowering phenotypes observed in *nox1*, WT, and *nos1* are consistent with the expression level of *FLC*, which suggests that endogenous NO may down-regulate the autonomous pathway, which results in late flowering.

Because previous studies have indicated the light-dependent nature of NO effects in plants, and *cue1* mutants show various defects in light perception and photomorphogenesis (*6*, *13*), we investigated whether NO regulates the photoperiod pathway. *Arabidopsis* is a facultative, long-day plant; long days promote flowering (*9*). *CONSTANS* (*CO*) is the most genetically downstream component of this pathway identified so far that promotes floral induction, and it acts as a link between the circadian clock and the control of flowering (*18*, *19*). SNP suppressed *CO* expression in a dose-dependent manner (Fig. 3, G and I). The *CO* expression was high in *nos1* but low in *nox1* plants compared with WT (Fig. 3, H and I). Consistently, *CO* and *FLC* expression were down- and up-regulated, respectively, in *cue1-5* plants (fig. S5). *CO* expression displays a diurnal rhythm (*18*); thus, the repression of *CO* by NO could be due to a reduction of amplitude, a phase shift, or both.

To quantify this effect of NO, we determined *CO* mRNA expression over a 12-hour light/12-hour dark cycle. The overall *CO* mRNA abundance was lower in *nox1* and higher in *nos1* than in WT, although the phase of *CO* mRNA level was not greatly disturbed (Fig. 4, A and B; fig. S6), consistent with previous studies on *gigantea* (*gi*) and *early flowering 3* (*elf3*), mutants of the photoperiod pathway (*20*, *21*). A *gi* lesion

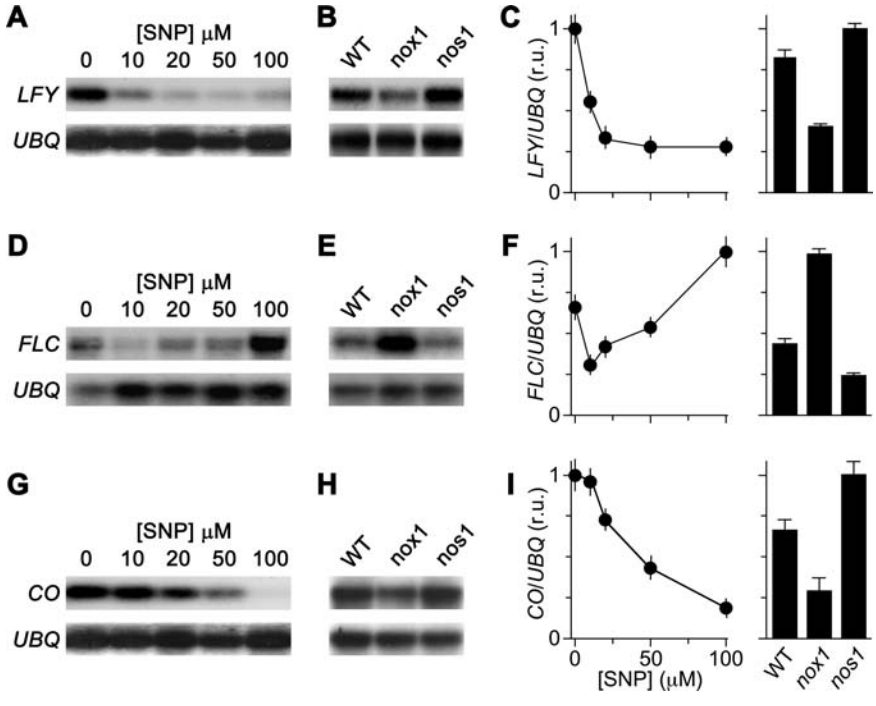

Fig. 3. NO affects the expression of genes that control the floral transition. (**A**, **D** and **G**) The effect of NO on the expression of *LFY*, *FLC*, and *CO*, respectively. Seedlings were grown in media containing SNP under long days. Leaves were collected 8 hours after dawn. The *LFY* and *CO* mRNA abundance was analyzed by using reverse transcription–polymerase chain reaction (PCR) and *FLC* mRNA by Northern blot (*10*). Ubiquitin mRNA (*UBQ*10) was used as a loading control. Similar results were seen for plants grown in 12-hour light/12-hour dark cycles. (**B**, **E**, and **H**) The expression levels of *LFY*, *FLC*, and *CO*, respectively, in WT, *nox1*, and *nos1* plants. Materials were prepared, and mRNA was analyzed as described in (A). (**C**, **F**, and **I**) Analysis of the effects of NO on *LFY*, *FLC*, and *CO* expression, respectively. The relative mRNA abundance was normalized to the *UBQ* levels. The maximum value was arbitrarily set to 1 (mean ± SEM; $n = 3$).

down-regulates *CO* expression, which results in late flowering, whereas an *elf3* lesion up-regulates *CO* expression, which leads to early flowering (*18*). To test whether NO directly affects *CO* expression, we analyzed *GIGANTEA* (*GI*), which is upstream of CO (*21*). The circadian amplitudes of *GI* mRNA abundance, similar to those of *CO*, were lower in *nox1* than WT (Fig. 4, C and D), which suggests that NO acts upstream of CO. Additionally, we analyzed the flowering phenotypes of *elf3* and *CO* overexpressing plants (*35S::CO*) (*22*) in response to NO. NO suppression of flowering was largely abolished in *elf3* mutants and *35S::CO* plants (Fig. 4F), which further supports the role of NO in the photoperiod pathway.

The expression of *CO* is regulated by the circadian clock and photoperiod, and the circadian rhythm of *CAB* expression can represent the circadian output in plants (*2*). The amplitudes of *CAB* mRNA abundance after switching from 12-hour light/12-hour dark cycles to continuous light for 3 days were greatly reduced in *nox1*, as well as in *cue1* mutants (*13*), whereas the circadian phases were not altered (*8*), similar to the expression of *CO* and *GI*. The amplitudes of another circadian output, cotyledon leaf movements, were also reduced by 43.8 ± 4.9% in *nox1* compared with WT, and no alteration of the circadian period was observed (Fig. 4E; fig S7). To analyze whether NO affects the circadian clock itself, we examined components of circadian clock central oscillators, *TIMING OF CAB EXPRESSION* (*TOC1*) and *CIRCADIAN CLOCK ASSOCIATED 1* (*CCA1*) (*23*, *24*). Neither the amplitude nor the circadian period of *TOC1* and *CCA1* expression was altered in *nox1* (*8*). Therefore, it is more likely that NO may affect circadian outputs rather than these central oscillators. Additionally, NO content in leaves in the middle of the night was 70.6% of that in the middle of the day in a 12-hour light/12-hour dark cycle for WT plants and 58.0% for *nox1* (table S2). This result suggests that the endogenous NO levels display a diurnal rhythm, consistent with a previous study (*7*). Although it is unclear whether NO production is dependent on light or the circadian clock, the alteration of NO homeostasis in *nox1* may cause its flowering phenotype.

We have provided pharmacological, physiological, molecular, and genetic data demonstrating that NO represses the photoperiod and autonomous floral pathways. These results are largely consistent with previous observations of delayed development in tobacco where NO is overproduced and of its inhibitory effects on maturation and senescence (*5*, *7*). Given that NO is induced by environmental changes, as well as constitutively produced, external and internal cues may converge on the regulation of endogenous NO status, which then relays these signals to the transcription regulatory network that controls the floral transition, which provides a unique layer of floral regulation. Oscillating NO levels, in addition to *CCA1* and *TOC*, may provide a mechanism to measure day/night switches, acting downstream of light perception to regulate certain circadian outputs and thus to control the floral transition, although the precise action of NO remains to be determined. Because several genes affected by NO (*CAB*, *CO*, and *GI*) are also regulated by light, the primary effect of NO may be on light signaling, and the effect on flowering may be secondary. Thus, identification of the direct target of NO will further our understanding of the molecular function of NO in plants.

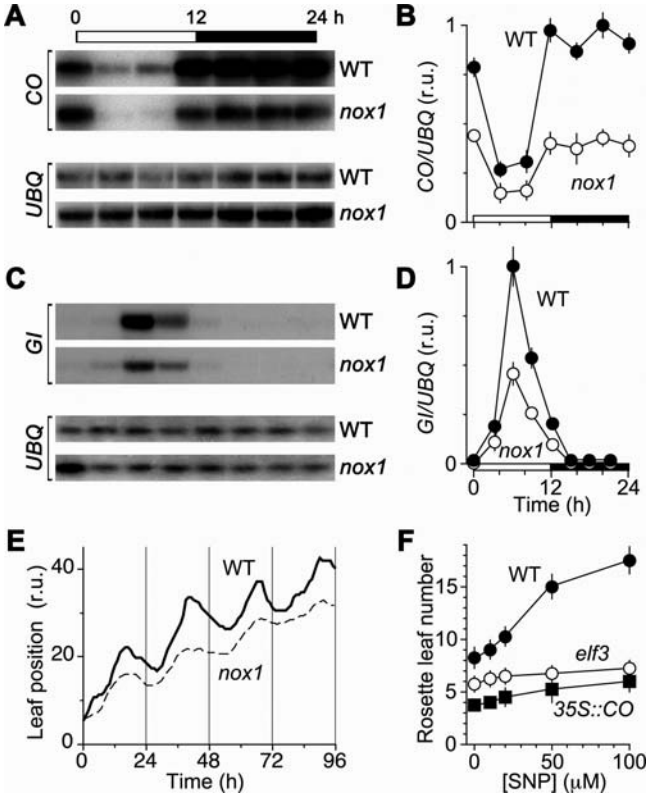

Fig. 4. NO suppresses the photoperiod pathway. (**A** and **C**) The mRNA abundance of *CO* and *GI* over a 24-hour time course. Plants were grown under 12-hour light/12-hour dark cycles for 10 days. Seedlings were collected every 4 hours for *CO* and every 3 hours for *GI* starting at dawn. The black and white bars at the top represent objective lights off and on, respectively. (**B** and **D**) Quantification of *CO* and *GI* mRNA abundance in (A) and (C), respectively (mean ± SEM; $n = 5$). (**E**) Circadian rhythms of cotyledon movements. Seedlings were grown under 12-hour light/12-hour dark cycles for 5 days, and cotyledon movements were recorded under constant dim light (*10*). (**F**) Analysis of the flowering time of *elf3* and *35S::CO* in response to SNP treatments (mean ± SD; $n = 150$ seedlings).

References and Notes

1. G. G. Simpson, C. Dean, *Science* **296**, 285 (2002).
2. A. Mouradov, F. Cremer, G. Coupland, *Plant Cell* **14**, S111 (2002).
3. H. H. Schmidt, U. Walter, *Cell* **78**, 919 (1994).
4. L. Lamattina, C. Garcia-Mata, M. Graziano, G. Pagnussat, *Annu. Rev. Plant Biol.* **54**, 109 (2003).
5. Y. Y. Leshem, E. Haramaty, *J. Plant Physiol.* **148**, 258 (1996).
6. M. V. Beligni, L. Lamattina, *Planta* **210**, 215 (2000).
7. Y. Morot-Gaudry-Talarmain *et al.*, *Planta* **215**, 708 (2002).
8. Y. He, Z.-M. Pei, data not shown.
9. M. Koornneef, C. J. Hanhart, J. H. van der Veen, *Mol. Gen. Genet.* **229**, 57 (1991).
10. Information on materials and methods is available on *Science* Online.
11. F.-Q. Guo, M. Okamoto, N. M. Crawford, *Science* **302**, 100 (2003).
12. M. R. Chandok, A. J. Ytterberg, K. J. van Wijk, D. F. Klessig, *Cell* **113**, 469 (2003).
13. H. Li, K. Culligan, R. A. Dixon, J. Chory, *Plant Cell* **7**, 1599 (1995).
14. S. J. Streatfield *et al.*, *Plant Cell* **11**, 1609 (1999).
15. M. A. Blazquez, L. N. Soowal, I. Lee, D. Weigel, *Development* **124**, 3835 (1997).
16. T.-p. Sun, F. Gubler, *Annu. Rev. Plant Biol.* **55**, 197 (2004).
17. S. D. Michaels, R. M. Amasino, *Plant Cell* **11**, 949 (1999).
18. P. Suarez-Lopez *et al.*, *Nature* **410**, 1116 (2001).
19. M. J. Yanovsky, S. A. Kay, *Nature* **419**, 308 (2002).
20. K. A. Hicks *et al.*, *Science* **274**, 790 (1996).
21. S. Fowler *et al.*, *EMBO J.* **18**, 4679 (1999).
22. H. Onouchi, M. I. Igeno, C. Perilleux, K. Graves, G. Coupland, *Plant Cell* **12**, 885 (2000) .
23. C. Strayer *et al.*, *Science* **289**, 768 (2000).
24. Z.-Y. Wang, E. M. Tobin, *Cell* **93**, 1207 (1998) .

25. We thank S. Han for assistance; Z. Mou and W. Wang for advice concerning map-based cloning; R. Fehon for use of a fluorescence stereomicroscope; R. Amasino for the *FLC* clone; G. Coupland for the *GI* clone and *35S::CO* seeds; *Arabidopsis* Biological Resource Center for *elf3* and *cue1* seeds; J. Chory, G. Coupland, J. Schroeder, X. Dong, and J. Dangl's lab for helpful discussion; and J. Siedow, T. Sun, P. Benfey, R. Fehon, P. Reeves, J. Reed, and R. Amasino for critical comments on the manuscript. Y.H. was supported by an exchange program between Duke University and Capital Normal University, Chinese NSF (30328003), and the Ministry of Science and Technology of China (2002AA2Z1001), and R.-H.T. by a Hargitt Fellowship. This work was supported by NSF (MCB-0132894), start-up funds, and Arts and Sciences Research funds from Duke University to Z.-M.P.

Supporting Online Material

www.sciencemag.org/cgi/content/full/305/5692/1968/DC1
Materials and Methods
Supporting Text
Figs. S1 to S7
Tables S1 and S2
Reference and Notes

6 April 2004; accepted 11 August 2004

Nitric oxide represses the *Arabidopsis* floral transition

Supporting Online Material

Contents

Materials and Methods

Plant material and growth conditions

All *Arabidopsis thaliana* genotypes used in the study are in Col-0 background. *cue1-1*, *cue1-5*, *cue1-6* and *elf3-1* were obtained from *Arabidopsis* Biological Resource Center, and *35S::CO*-containing seeds were a kind gift from Dr. G. Coupland. *Arabidopsis* plants were grown in soil (Scotts Metro-Mix 200), or in petri dishes (100 x 15 mm) and Magenta vessels (77 mm x 77 mm x 97 mm; sigma) in half-strength MS media (Gibco), 1% (w/v) sucrose (Sigma), 0.8% (w/v) agar (Becton Dickinson) in controlled environmental rooms at ~22 °C and at a photon fluency rate of ~100 μmol m^{-2} sec^{-1}. The photoperiods were 16 h light/8 h dark cycles for long days and 8 h light/16 h dark cycles for short days. Plants were also grown in 12 h light/12 h dark cycles as

indicated. For circadian experiments, plants were grown in petri dishes under 12 h light/12 h dark cycles for about 10 days and then transferred to continuous light at dawn (*1, 2*). Sodium nitroprusside (SNP, Sigma) at concentrations indicated was added in the MS media. The absolute NO concentrations in petri dishes (Fig. 1A) and Magenta vessels (Fig. 2G) differed due to differences in total volumes.

Analysis of flowering time

It has been shown that flowering time is closely related to the number of leaves produced on the primary stem before the first flower is initiated, and late-flowering plants form more leaves (*3*). For soil-grown plants we scored the number of rosette leaves and days to flowering at the stage when the first flower was appearing (*2, 4, 5*). For seedlings grown in MS media in petri dishes, because it was difficult to score the number of leaves at the stage of flowering, we scored the number of rosette leaves at the stage of bolting when stems were about 3 mm, as performed previously (*6*). We also scored days to bolting.

Isolation of NO overproducing mutants

For the genetic screen, fast neutron-mutagenized *Arabidopsis* (Col-0) seeds were obtained from Lehle Inc. These seeds were plated on half-strength MS media containing 1% sucrose, 0.8% agar, and 10 μM SNP for 5 days. Seedlings with very small roots were selected as putative *NO overproducer* (*nox*) mutants, and transplanted to SNP-free media for 7 days and then to soil to obtain seeds. Putative *nox* mutants were stained with an NO sensitive dye, 4,5-diaminofluorescein diacetate (DAF-2DA) as described bellow, and *nox* mutants were obtained. Further analysis of root growth in response to SNP and genetic analysis were conducted to confirm isolated mutants (fig. S3).

Analysis of the levels of NO

The endogenous NO levels were analyzed using an NO-sensitive dye, 4,5-diaminofluorescein diacetate (DAF-2DA) (*7-10*) or an NO-selective electrode (*11, 12*). For DAF-2DA imaging, *Arabidopsis* seedlings were grown in soil under long days. Rosette leaves were collected 8 hours after dawn, incubated in a solution containing 0.1 mM $CaCl_2$, 10 mM KCl, 10 mM MES-Tris, pH 5.6 for 2 h, and stained with 10 μM DAF-2DA (Molecular Probe) for 45 min. These leaves

were analyzed using a fluorescence stereomicroscope (MZ FLIII, Leica) equipped with a CCD camera. The excitation was provided at 495 nm and the emission images at 515 nm were obtained with a constant acquisition time.

For quantitative analysis of NO content in plants, plants were grown in soil under 12 h light/12 h dark cycles, and rosette leaves were collected 6 hours after dawn unless described elsewhere. 0.5 g leaves were frozen using liquid nitrogen, ground, and resuspended in a solution (1.5 mL) containing 0.1 mM $CaCl_2$, 10 mM KCl, 10 mM MES-Tris, pH 5.6. The concentration of NO in aqueous solutions was measured using an ISO-NO Mark II NO meter (World Precision Instruments) connecting to an amperometric electrode according to the manufacturer's instructions (*13, 14*). Calibration of the NO electrode was performed prior to each experiment. The standard calibration curve was generated by the aqueous standards prepared with NO gas (*13, 14*). The concentration of saturated NO stock solution is 2 mM at 22 ºC. NO concentration was measured and analyzed using the Duo 18 data acquisition system (World Precision Instruments) connected to a PC computer.

Analysis of the content of L-arginine and L-citrulline

The leaf materials were prepared as described (*15*). The concentrations of free amino acids were determined by isotope dilution tandem mass spectrometry after derivatization to butyl esters and employing positive neutral loss scans of 119 and 161 Da for L-citrulline and L-arginine, respectively as described (*16*). Measurements were made using a Quattro LC triple quadrupolar mass spectrometer (Micromass) as described (*17*).

Positional identification of *nox1*

We back-crossed *nox1* to WT (Col-0) three times. The homozygous *nox1* line in the Col-0 background was crossed to the polymorphic ecotype L*er* and followed by self-pollinating F1 progeny to yield an F2 mapping population of 1,598 chromosomes. Linkage analysis of F2 plants was revealed that the *nox1* locus locates in chromosome 5. Fine mapping markers were chosen using http://*Arabidopsis*.org, MapViewer Home. These markers were used to perform PCR and isolated the interval that flanks the mutation. When we used the marker, *CUE1*, to map *nox1*, no recombinants were found. Finally, we confirmed that *NOX1* is *CUE1* (see fig. S3 and text for details).

Analysis of *LFY*, *FLC* and *CO* mRNA abundance

The abundance of *LFY* and *CO* mRNA was analyzed using reverse transcription polymerase chain reaction (RT-PCR), as described (*2, 18*). For *LFY*, *CO* and *FLC* expression at a single time point (Fig. 3), wild type, *nox1* and *nos1* plants were grown side-by-side in petri dishes in MS-media for 10 to 16 long days. Shoots were collected 8 hours after dawn. Messenger RNAs were prepared and reverse transcribed using a cDNA synthesis kit according to the manufacturer's instructions (Invitrogen). Primers used for the PCR reactions were as follows: *LFY*, 5'-tcatttgctactctccgccgct, 5'-catttttcgccacggtctttag; *CO*, 5'-cattaaccataacgcatacatttc, 5'-ctcctcggcttcgatttctc; *UBQ10*, 5'-taaaaactttctctcaattctctct, 5'-ttgtcgatggtgtcggagctt. For PCRs, 25 cycles were used for *LFY* and *CO*, and 20 cycles for *UBQ10*. Primers for *CO*, *UBQ10* and *LFY* were described by Putterill et al. (*19*), Wang and Tobin (*20*), and Chou et al. (*18*), respectively. PCR products were detected by standard Southern blot using radioactively labeled probes. *FLC* mRNA abundance was detected using standard Northern blot as described (*4, 21*) with a probe made from a *FLC* clone (a gift form Dr. R. Amasino). Total RNA (10 µg) was electrophoresed, transferred to Hybridization Transfer Membrane (PerkinElmer), and blotted with radioactively labeled probes. Expression levels were normalized against the signal obtained by hybridizing the same blot or same RT-PCR samples with an *UBQ10* probe. The abundance of mRNAs was further analyzed using PHOTOSHOP 6.0. Similar results were seen at least in three independent experiments.

Analysis of circadian expression of *CO*, *GI*, *CAB*, *TOC1* and *CCA1*

Wild type and *nox1* plants were grown side-by-side in petri dishes for about 10 days at 12 h light/12 h dark cycles, and moved to continuous white light. Every 4 h for *CO*, or 3 h for *GI*, *CAB*, *TOC1* and *CCA1*, shoots from five plants were pooled for RNA extraction. Analysis of *CO* mRNA abundances was conduced as described above using RT-PCR. Analysis of *GI*, *CAB*, *TOC1* and *CCA1* mRNA abundances was conduced using standard Northern blot as described above. The probes for *GI* was described by Fowler et al. (*22*), *CAB* and *CCA1* by Wang et al. (*20*), and *TOC1* by Alabadi et al. (*23*), *UBQ10* by Jarillo et al. (*1*). The *GI* clone was a kind gift from Dr. G. Coupland. Similar results were seen at least in three independent experiments.

Analysis of circadian cotyledon movements

Circadian cotyledon movements were analyzed as described previously (*1, 24*). *Arabidopsis* seeds were surface-sterilized and sown in two rows, one of *nox1* and one of the wild type on ½ MS medium containing 1% sucrose. The seeds were incubated in petri dishes under 12 h light/12 h dark cycles for 5 days. The petri dishes were placed before a SONY video camera (DCR-TRV240), and cotyledon movements were recorded under continuous white light. We recorded the position of cotyledon tips for 96 h as described previously (*1, 24*). All statistical analyses were performed using EXCEL 9.0 (Microsoft) and data were presented as described (*25, 26*). Values of $P < 0.05$ were considered statistically significant.

Supporting Text

NO represses the photoperiod and the autonomous pathways

The repression of the photoperiod pathway by NO is supported by several findings reported here that the level of NO was negatively correlated with the expression of *CO* and *GI*; the *elf3* lesion and *CO* overexpression disrupted the NO effects on flowering; and that the circadian amplitudes of cotyledon leaf movements and *CAB* mRNA were reduced in *nox1* mutants, as well as by previous observation that *cue1* exhibits lower responsiveness to phytochrome signals and delayed chloroplast development (*15, 27*). Additionally, several lines of evidence suggest that NO may also repress the autonomous pathway, including that exogenously-applied NO altered the expression of *FLC*; the level of *FLC* mRNA was correlated with the flowering phenotype of *nox1*, *cue1*, and *nos1*; and that *nox1* flowered late in both long and short days, a characteristic of mutants of the autonomous pathway. Thus, we conclude that NO has a specific role in the control of flowering although its action is not limited to flowering (*10*). To our knowledge, plant growth regulators other than NO, which repress the floral transition opposite to GA, and regulate the expression of signaling components in the floral pathways, such as *CO*, *FLC* and *LFY*, have not been documented and characterized to date.

NO regulates uniquely circadian outputs in plants

It has been well established that light quality and day length regulate circadian rhythms (*28, 29*), while regulation of circadian rhythms by environmental and physiological signals other than

light (*30*) has not yet been well characterized in plants. In contrast, in animals signals such as food and redox states have been implicated in circadian rhythm regulation, and the role of NO has been suggested (*28*). Based on our findings and a previous report (*31*) we propose a working model, in which day and night changes result in the diurnal rhythm of the levels of NO *in vivo*, and the circadian NO status functions downstream of light perception to control clock-regulated processes in *Arabidopsis*. Therefore, the regulation of circadian outputs by NO may represent a potential mechanism by which NO represses the floral transition.

Physiology relevance of NO repression of flowering

We propose further that the repression of flowering by NO provides a previously unknown physiological mechanism by which plants fine-turn their growth and development to their micro-environmental conditions. The dramatic flowering phenotypes in *Arabidopsis* often seen in naturally occurring ecotypes largely reflect the adaptation of plants to major environmental factors such as seasonal changes (*32*). The relatively week flowering phenotypes seen in *nox1* and *nos1* may reflect the adaptation of plants to minor environmental changes, such as water and salt status or pathogen infection, as these external factors have been shown to alter the status of endogenous NO in plants (*10, 33*). Additionally, given that NO is also constitutively produced in plants (*8, 10, 33*), it is likely that both internal and external cues converge on the regulation of endogenous NO status, which then relays these signals to the transcription regulatory network (*30, 32*) that controls the floral transition, providing a unique regulatory mechanism for the floral transition.

Figure S1. Nitric oxide promotes vegetative growth but inhibits reproductive development.

(**A**) *Arabidopsis* seedlings were grown in media containing MS salts, 1% sugar, 0.8% agar and SNP at concentration indicated for five weeks.

(**B**) Average fresh-weight per root plotted as a function of the applied SNP concentrations from experiments as in (A). Data from four separate experiments with duplicates are presented as the mean ± SD. (n = 150 seedlings).

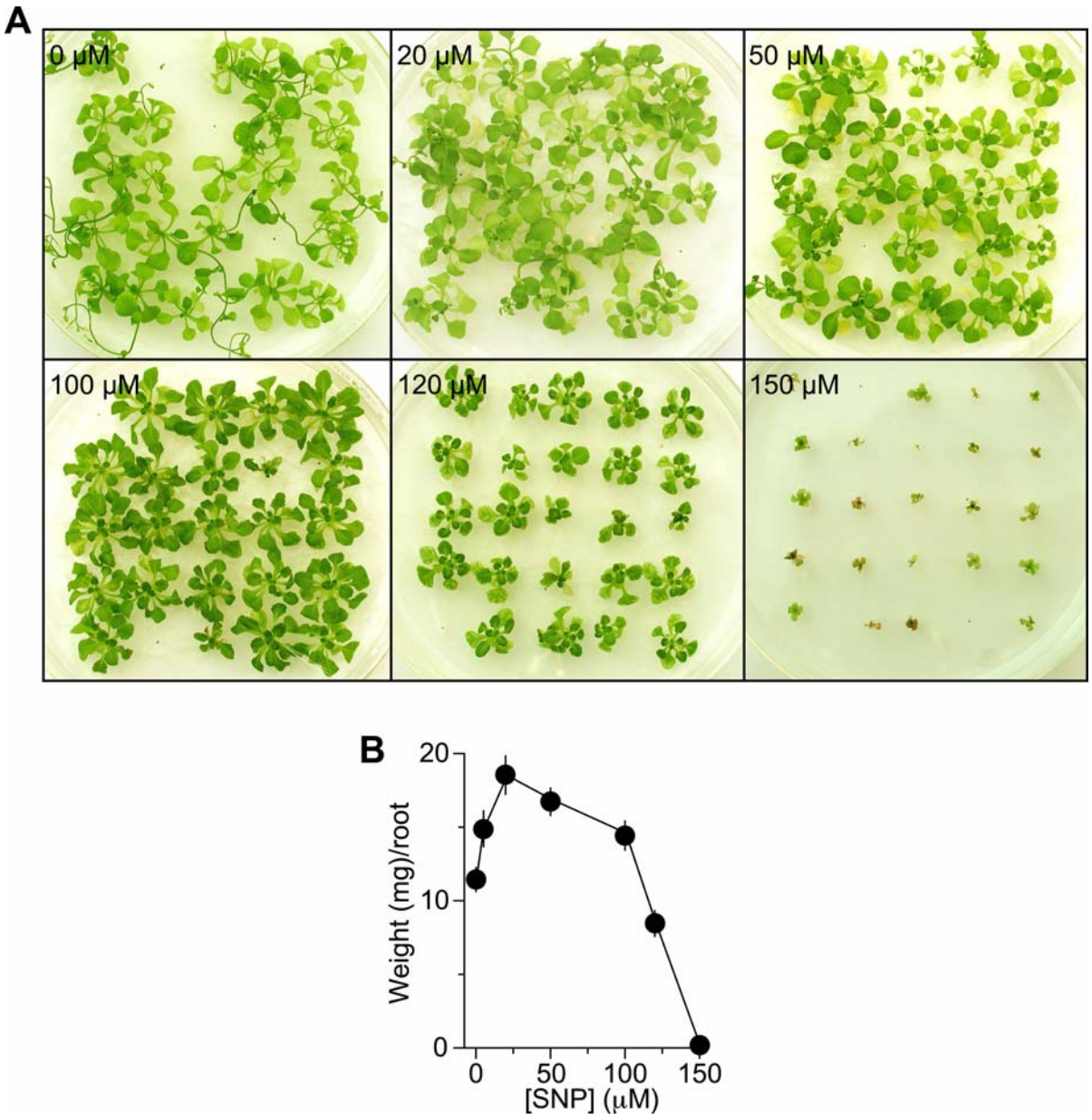

Figure S2. The *nox1* phenotype of root growth hypersensitive to SNP.

Quantitative analyses of the *nox1* root growth in response to SNP. Wild type (WT) and *nox1* seedlings were grown in MS media containing several concentrations of SNP for 5 days. Root length was plotted as a function of applied concentrations of SNP. Log-scale is used for the concentration of SNP (mean ± SD; n = 60 seedlings).

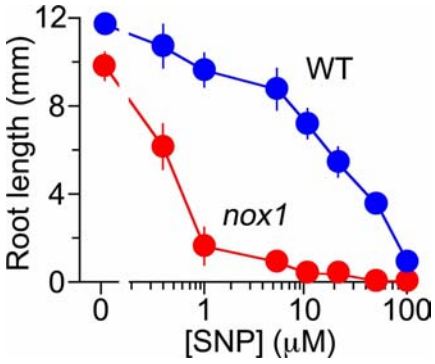

Figure S3. Map-based cloning reveals that *NOX1* is identical to *CUE1*.

(A) *NOX1* was mapped to a region close to centromer of chromosome 5 by analyzing 1,598 recombinant chromosomes from F2 seedlings derived from a *nox1* x L*er* cross with molecular markers. When the marker *CUE1* was used, zero recombinant chromosomes/1,598 were found, suggesting that *NOX1* might be *CUE1* (*15, 27*).

(B) *nox1* and *cue1* mutants displayed similar hypersensitivity to SNP. The experimental conditions were the same as in Figure 2A. Similar results were obtained in 6 independent experiments (n = 180 seedlings).

(C) Genetic analysis shows that *NOX1* is identical to *CUE1*. All F1 seedlings derived from a *nox1* x WT cross showed root growth insensitive to 5 μM SNP. F2 seedlings showed a 3:1 WT:*nox1* segregation (*34*), suggesting that *nox1* is a recessive mutation. All F1 seedlings derived from a *nox1* x *cue1-5* cross showed a *nox1* phenotype in root growth, suggesting that *nox1* is identical to *cue1*. The *cue1-5* mutant harbors a single amino acid mutation (*15*).

(D) *cue1-5* overproduces NO. The experiments were carried out as described in Figure 2B using an NO sensitive dye DCF-2DA (top). White-light photographs with reticulate patterns similar to *nox1* (Fig. 2B bottom) are shown at bottom. Total of 60 leaves were analyzed for WT or *cue1-5* in 3 independent experiments, and similar resulted were obtained.

(E) *CUE1* is deleted in *nox1* mutants. PCR analysis shows that *CUE1* was deleted in *nox1-1*, *nox1-2*, and *cue1-1*, but not in WT and two *cue1* mutants, *cue1-5* and *cue1-6*, carrying a point mutation. The primers for *CUE1* analyses were 5'-tctcgttctgatggctcctgtg and 5'-gtgtaaccggtgatactctcgcc.

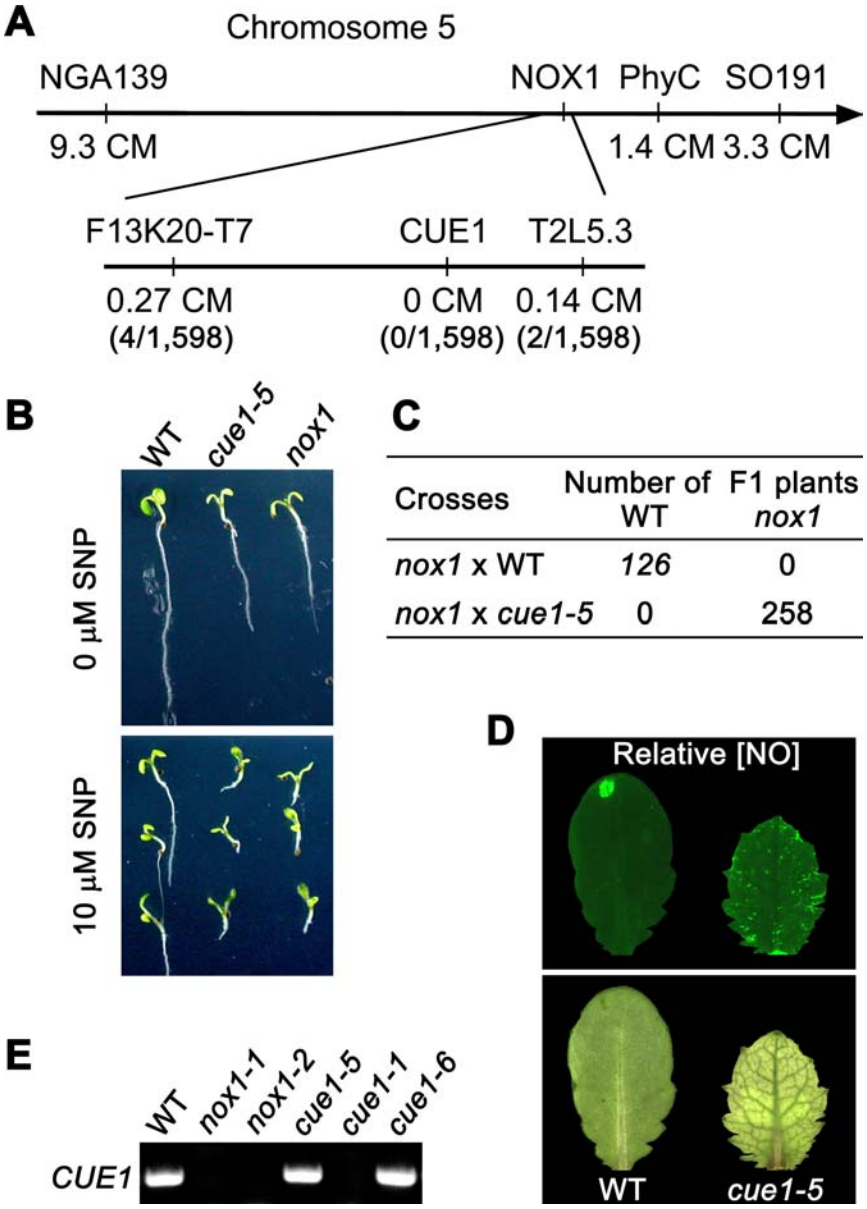
A
Chromosome 5
NGA139
NOX1
PhyC
SO191
9.3 CM
1.4 CM
3.3 CM
F13K20-T7
CUE1
T2L5.3
0.27 CM
(4/1,598)
0 CM
(0/1,598)
0.14 CM
(2/1,598)
B
WT
cue1-5
nox1
0 µM SNP
10 µM SNP
C
Crosses
Number of F1 plants
WT
nox1
nox1 x WT
126
0
nox1 x cue1-5
0
258
D
Relative [NO]
WT
cue1-5
E
WT
nox1-1
nox1-2
cue1-5
cue1-1
cue1-6
CUE1

Figure S4. The contents of L-citrulline in wild type, *nox1* and *cue1* mutants. The content of NO was measured using an NO-sensitive electrode as described in Materials and Methods. Values are normalized to that of wild type (20.0 nmol per gram fresh-weight of rosette leaves). Each data point represents 9 independent measurements.

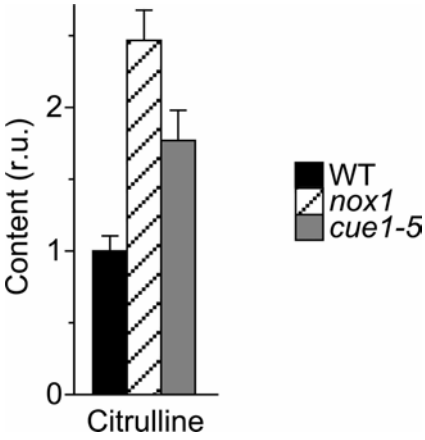

Figure S5. The expression of *FLC* and *CO* in *cue1-5* plants. The *cue1-5* mutants showed elevated *FLC* mRNA abundance and reduced *CO* mRNA abundance, consistent with these in *nox1* plants. Seedlings were grown in MS media containing 16 h light/8 h dark cycles. Leaves were collected 8 hours after dawn. The *CO* mRNA abundance was analyzed using reverse transcription-PCR. The *FLC* mRNA abundance was analyzed by Northern blot. Ubiquitin mRNA (*UBQ10*) was used as a loading control. Similar results were seen in three independent experiments.

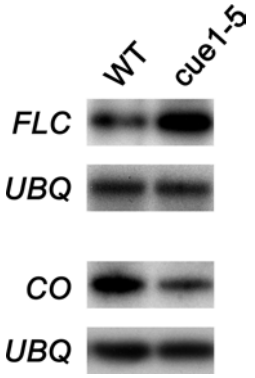

Figure S6. The enhanced circadian amplitudes of *CO* expression in *nos1* mutants. The overall mRNA abundances of *CO* over a 24-hour time course were slightly yet consistently higher in *nos1* plants than in wild type. Seedlings were grown in petri dishes under 12 h light/12 hr dark cycles for 10 days, and collected every 4 h starting at dawn over a 24-hour time course. The black and white bars at the top represent objective lights off and on, respectively. Other conditions were the same as in Fig. 4A. Data are the mean ± SEM (n = 3).

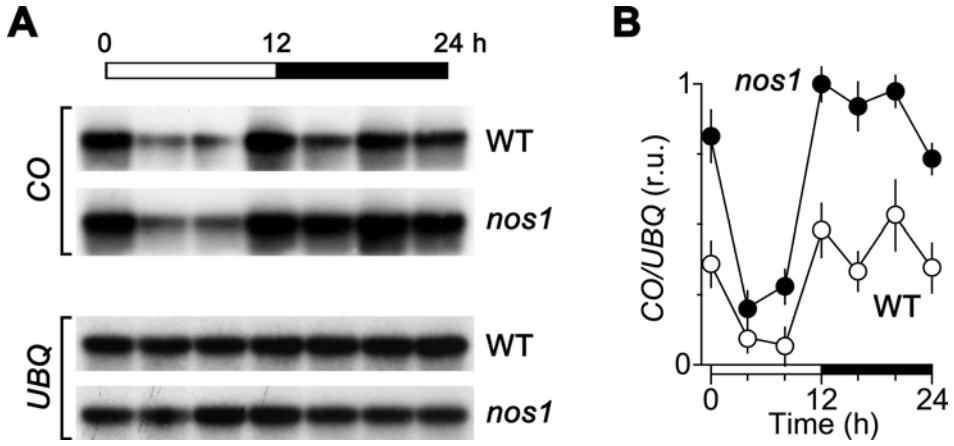

Figure S7. The reduced circadian amplitudes of cotyledon movements in *nox1* mutants. Seedlings were entrained in 12 h light/12 h dark cycles and transferred to constant light as described in Materials and Methods. Cotyledons at the up position and the low position were illustrated for wild type and *nox1* seedlings from experiments as in Fig. 4E. The smaller circadian amplitudes of cotyledon movements in *nox1* seedlings (Fig. 4E) were not attributed to its relatively slow growth, but to its lesser closure of cotyledons. The angle of *nox1* cotyledons was larger than that of wild type at the up position, while the angle similar to that of wild type was seen in the low position in *nox1*.

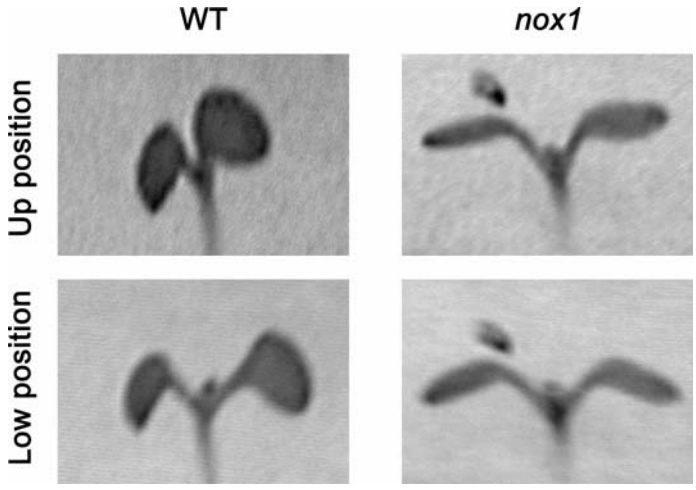

Table S1. Flowering time of *nox1* and *cue1-5* plants. Flowering time is presented as the number of rosette leaves formed on the main stem, and late-flowering plants form more leaves (*3*). At least 25 plants of each genotype were examined. Flowering time was also scored by the number of days from sowing until the first flower was visible.

	Rosette leaf number*			Days to flowering*		
	16 h/8 h†	12 h/12 h	8 h/16 h	16 h/8 h	12 h/12 h	8 h/16 h
Wild type	12.3 ± 0.5	18.6 ± 0.9	47.6 ± 2.3	33.2 ± 1.2	46.5 ± 2.6	98.5 ± 5.9
nox1	14.5 ± 0.6	29.9 ± 1.2	55.8 ± 3.4	42.6 ± 1.5	75.2 ± 2.3	153.8 ± 8.3
cue1-5	18.1 ± 1.2	28.8 ± 2.3	ND	39.6 ± 2.5	71.9 ± 3.4	ND

* mean ± SD † 16 h/8 h, 16 hour light/ 8 hour dark cycles. ND, not determined.

Table S2. The diurnal rhythm of the content of NO in *Arabidopsis* leaves. Since we found the changes in circadian amplitudes in response to NO, we wondered whether the endogenous NO levels also display a diurnal rhythm. A previous study has shown that the emission of NO from tobacco plants exhibits 'typical circadian cycles,' being several fold higher in the light than in the dark (*31*). Nevertheless, the diurnal rhythm of NO emission from plants may be attributed to a diurnal rhythm in endogenous NO status or circadian rhythms of stomatal conductance, as stomata open in the day and close at night. Our result suggests that the endogenous NO levels display a diurnal rhythm, possibly independent of stomatal conductance. Seedlings were grown under 12 h light/12 hr dark cycles. Rosette leaves were collected in the middle of the day or the middle of the night, and the content of NO was measured using an electrode-based method described in the Materials and Methods. Data are the mean ± SEM (n = 9).

	The content of NO in *Arabidopsis* leaves (pmol per gram fresh-weight)			
	in the middle of the day	in the middle of the night	% (night/day)	*P* value
Wild type	449 ± 19	317 ± 18	76.6	< 0.0001
nox1	895 ± 15	519 ± 17	58.0	< 0.0001

References and Notes

1. J. A. Jarillo *et al.*, *Nature* **410**, 487 (2001).
2. P. Suarez-Lopez *et al.*, *Nature* **410**, 1116 (2001).
3. M. Koornneef, C. J. Hanhart, J. H. van der Veen, *Mol Gen Genet* **229**, 57 (1991).
4. S. D. Michaels, R. M. Amasino, *Plant Cell* **11**, 949 (1999).
5. M. A. Blazquez, L. N. Soowal, I. Lee, D. Weigel, *Development* **124**, 3835 (1997).
6. M. J. Yanovsky, S. A. Kay, *Nature* **419**, 308 (2002).
7. I. Foissner, D. Wendehenne, C. Langebartels, J. Durner, *Plant J* **23**, 817 (2000).
8. F.-Q. Guo, M. Okamoto, N. M. Crawford, *Science* **302**, 100 (2003).
9. M. R. Chandok, A. J. Ytterberg, K. J. van Wijk, D. F. Klessig, *Cell* **113**, 469 (2003).
10. L. Lamattina, C. Garcia-Mata, M. Graziano, G. Pagnussat, *Annu Rev Plant Biol* **54**, 109 (2003).
11. J. Schnermann, D. Z. Levine, *Annu Rev Physiol* **65**, 501 (2003).
12. C. D. Reiter *et al.*, *Nat Med* **8**, 1383 (2002).
13. X.-J. Zhang, L. Cardosa, M. Broderick, H. Fein, *Free Radical Bio Med* **27**, S89 (1999).
14. X.-J. Zhang, L. Cardosa, M. Broderick, H. Fein, J. Lin, *Electroanal* **12**, 1113 (2000).
15. S. J. Streatfield *et al.*, *Plant Cell* **11**, 1609 (1999).
16. D. S. Millington, N. Kodo, N. Terada, D. Roe, D. H. Chace, *Int J Mass Spectrom Ion Processes* **111**, 211 (1991).
17. C. Bonaventura *et al.*, *Biophys Chem* **98**, 165 (2002).
18. M.-L. Chou, M.-D. Haung, C.-H. Yang, *Plant Cell Physiol* **42**, 499 (2001).
19. J. Putterill, F. Robson, K. Lee, R. Simon, G. Coupland, *Cell* **80**, 847 (1995).
20. Z.-Y. Wang, E. M. Tobin, *Cell* **93**, 1207 (1998).
21. Y.-H. He, S. D. Michaels, R. M. Amasino, *Science* **302**, 1751 (2003).
22. S. Fowler *et al.*, *EMBO J* **18**, 4679 (1999).
23. D. Alabadi *et al.*, *Science* **293**, 880 (2001).
24. M. J. Dowson-Day, A. J. Millar, *Plant J* **17**, 63 (1999).
25. Z.-M. Pei, M. Ghassemian, C. M. Kwak, P. McCourt, J. I. Schroeder, *Science* **282**, 287 (1998).
26. Z.-M. Pei, K. Kuchitsu, J. M. Ward, M. Schwarz, J. I. Schroeder, *Plant Cell* **9**, 409 (1997).
27. H. Li, K. Culligan, R. A. Dixon, J. Chory, *Plant Cell* **7**, 1599 (1995).

28. J. Rutter, M. Reick, S. L. McKnight, *Annu. Rev. Biochem.* **71**, 307 (2002).
29. D. E. Somers, P. F. Devlin, S. A. Kay, *Science* **282**, 1488 (1998).
30. A. Mouradov, F. Cremer, G. Coupland, *Plant Cell* **14**, S111 (2002).
31. Y. Morot-Gaudry-Talarmain *et al.*, *Planta* **215**, 708 (2002).
32. G. G. Simpson, C. Dean, *Science* **296**, 285 (2002).
33. S. J. Neill, R. Desikan, J. T. Hancock, *New Phytol* **159**, 11 (2003).
34. Y. He, Z.-M. Pei, data not shown.

Supporting Online Material

www.sciencemag.org

Materials and Methods

Supporting Text

Figs. S1 to S7

Table S1 and S2

Reference and Notes